glacies

MDPI

Article

Glacial Thrusts: Implications for the Crustal Deformation of the Icy Satellites

Costanza Rossi [1,*], Riccardo Pozzobon [2], Mateo Martini [3], Eliseo Flores [3], Alice Lucchetti [1], Maurizio Pajola [1], Luca Penasa [1], Giovanni Munaretto [1], Filippo Tusberti [1] and Joel Beccarelli [1]

[1] National Institute for Astrophysics (INAF)—Astronomical Observatory of Padova, 35122 Padova, Italy
[2] Department of Geoscience, University of Padova, 35122 Padova, Italy
[3] Centro de Investigaciones en Ciencias de la Tierra (CICTERRA, CONICET), University of Córdoba, Córdoba 5000, Argentina
* Correspondence: costanza.rossi@inaf.it

Abstract: The icy satellites of the outer Solar System show surfaces strongly deformed by tectonic activity, which mostly shows wide strike-slip zones. The structural pattern recognized on such regions can be ascribed to the deformation observed on terrestrial analogs identified in glaciers, whose flow produces deformation structures that bear key information to compare and better understand the surface and subsurface development of the structures identified on icy satellites. Multiscale analysis is used to acquire local- and regional-scale datasets that are compared with icy satellite data. Glacier deformation structures are compared with those identified in a unique regional-scale investigation of the icy satellites. In this work, we present a review of the approach used for the comparison between glacial and icy satellite shear zone deformation. The comparison concerns the deformation styles observed in these bodies, with a particular emphasis on compressional structures, called thrusts, which are hardly detected on icy satellites. Thrusts occur on glaciers and are important for glacial flow, deformation compensation and fluid circulation. Here, we report the occurrence of glacial thrust to better understand the icy environment under deformation and make inferences on icy satellite shear zones. Thanks to fieldwork and remote sensing analyses, we can infer the potential location and development of such compressional structures on icy satellites, which are pivotal for the compensation of their tectonics. We analyze glacial deformation by considering the icy satellite context and we discuss their potential detection with data from current and future planetary missions. A total of five categories of thrusts are presented to understand the best method for their detection, and a conceptual model on icy satellite surface and subsurface structural pattern is proposed.

Keywords: thrust faulting; glacier deformation; icy satellites; tectonics

check for updates

Academic Editor: Steven R. Fassnacht

Received: 29 October 2024
Revised: 12 February 2025
Accepted: 3 March 2025
Published: 10 March 2025

Citation: Rossi, C.; Pozzobon, R.; Martini, M.; Flores, E.; Lucchetti, A.; Pajola, M.; Penasa, L.; Munaretto, G.; Tusberti, F.; Beccarelli, J. Glacial Thrusts: Implications for the Crustal Deformation of the Icy Satellites. *Glacies* **2025**, *2*, 4. https://doi.org/10.3390/glacies2010004

Copyright: © 2025 by the authors. Licensee MDPI, Basel, Switzerland. This article is an open access article distributed under the terms and conditions of the Creative Commons Attribution (CC BY) license (https://creativecommons.org/licenses/by/4.0/).

1. Introduction

Water ice is widespread across the Solar System. From Earth to the gas giant systems, ice occurs as ice sheets and permafrost on rocky planets and in different phases; it can even comprise the entire crust of solid bodies, such as the icy satellites of Jupiter, Saturn and Uranus [1].

Solid water can occur in at least 15 different crystalline forms of ice that pack more densely according to variations in pressure and temperature [2]. Except for the low-pressure form ice-*Ih*, which is the ordinary 0.92 g/cm^{-3} hexagonal water ice naturally occurring on Earth at 0 °C and standard atmospheric pressure, and a small percentage

of ice-*Ic*, i.e., the metastable cubic crystalline variant of low-pressure ice that can occur in the atmosphere [2,3], the other forms have only been recreated in laboratory experiments; however, it is assumed that they can occur in the interior of icy bodies of the outer Solar System [4–6]. Such forms are the high-pressure forms ice-II, -III, -V, -VI, -VII, -VIII, -IX, -X (1.66 g/cm^{-3}), the metastable forms ice-IV and -XII and the low-pressure and low-temperature ice-XI [6]. The crystalline phases of water ice can incorporate in their lattice volatiles such as methane, nitrogen, CO_2, and noble gases. These cage-like structures are called clathrate hydrates and are found on Earth's glaciers, permafrost and seafloor sediments [7].

Moreover, water can also solidify in amorphous ice forms, which lack molecular arrangement due to the rapid cooling of liquid water or due to compression of the ordinary ice-*Ih* at low temperatures [8]. Amorphous ice is present in outer space, but is not common on Earth's surface, although it is thought to occur in the upper atmosphere [2].

The icy satellites are characterized by a variety of such phases, from the low-pressure ice at the surface to a phase transition at depth into high-pressure ice forms [9]. In this way, the upper portion of their crust, including their surface, is composed of *ice-Ih* [5,10]. Cubic ice has also been suggested as a component of the surface of the icy satellites by a few authors (e.g., [11]), but its molecular structure, which consists of alternating hexagonal and cubic layers, in time gradually transforms into hexagonal ice. In addition, amorphous ice has been suggested to occur at the surface of icy satellites as well as clathrate hydrates [11,12]. However, their spatial distribution does not encompass the entire surface but is clustered in scattered areas. For this reason, most authors (e.g., [4,5,13]) consider that the surface of the icy satellites is mostly composed of ice-*Ih*. For this reason, this work focuses on polycrystalline ordinary ice.

Similarly to rocks, ice-*Ih* is a solid material whose behavior changes in response to stress by deformation mechanisms [14,15]. It experiences permanent deformation, depending on parameters, such as temperature, pressure and grain size [16–20]. Consequently, the occurrence of deformation structures is controlled by (i) brittle and (ii) ductile regimes [14,21–23]. (i) In the brittle regime, ice displays elastic and/or plastic behavior at relatively high strain rates and relatively cold temperatures due to localized brittle failure, which is accompanied by the growth of fractures and faults. (ii) At high temperatures, distributed ductile deformation dominates, which is represented by plastic behavior that manifests uniform flow in which no loss of cohesion across a discrete surface occurs [24].

Ice dynamics plays a crucial role in both terrestrial and extraterrestrial bodies. On Earth, glaciers and ice sheets are active components that show intense deformation. Driven by gravity, glaciers flow and deform due to the stresses exerted by their weight [19]. According to the velocity, the temperature and the underlying bedrock topography, the glacier's kinematics induce a predictable structural pattern. At the surface, brittle structures (crevasses, fractures, faults) form and tend to disappear at depth, where ductile processes control the formation of folds and basal detachments that allow the flow of the icy mass [25]. The glacial dynamics can represent a small-scale structural model for rock deformation [14]. Similar to crustal rocks, glaciers show a structural and rheological variation from the brittle surface to the ductile depth. Moreover, their structural patterns can be an analog for the deformation in orogenic belts, responsible for mountain formation, or for shear zones, where strike-slip governs the horizontal displacement of crustal blocks [25–27]. Active ice masses also represent optimal terrestrial analogs for the tectonic investigation of the outer Solar System icy satellites.

The icy satellites are solid bodies that orbit the giant planets, and their crust is composed of ice (from the low-pressure ice-*Ih* at the surface to the high-pressure phases at depth [5,9,10]). These are active bodies that show icy surfaces strongly deformed by tec-

tonic processes [28]. Deformation structures pervade their surfaces, e.g., from the Jovian Europa and Ganymede to the Saturnian Enceladus and Dione [29–32]. At a regionalscale, kilometer-long linear to curvilinear brittle structures exhibit puzzling patterns, mostly related to extensional and strike-slip tectonics [33–40]. On the other hand, the scarcity of compressional structures represents a structural geology enigma. The observed amount of crustal extension and shear requires accommodation and compensation by a similar or equivalent amount of compression, which is not observed in regional-scale investigations. The main structural patterns recognized on icy satellite surfaces are represented by extensional *horst and graben* settings, which are alternations of valleys and ranges [41,42], and the strike-slip shear zones, also known as shear corridors [43,44]. The latter are characterized by a couple of long and nearly parallel strike-slip faults that delimit an elongated area containing shorter subsidiary structures associated with the deformation induced by the kinematics of regional shear [43]. The strike-slip zone setting can be ascribed to what is observed on glaciers.

In this way, glaciers and their deformation style provide a close analogy with what is identified on icy satellites and support their geological and tectonic analysis. Despite the differences, it is possible to compare the deformation patterns that these bodies show. In fact, the processes responsible for the structure formation and their respective timescales cannot be considered, as the collected data in this work do not provide sufficient criteria to constrain the comparison between the deformation processes of glaciers and those of icy satellite surfaces (i.e., ice mass kinematics vs. geodynamical processes, respectively). Glaciers are unconfined masses lying above the bedrock surface and flowing due to gravity. On the other hand, icy satellites are characterized by confined crusts that often lie above an ocean (located thousands or tens of thousands of kilometers deep). Therefore, the comparison focuses on their deformation patterns, which contribute to constraining the deformation styles in the brittle crusts of icy satellites and inferring the structural network that develops at depth.

Since the comparison concerns the understanding of the deformation pattern in the upper portion of the icy satellite crusts, this work considers glacier kinematics as the primary analog for shear zones recognized on the icy satellites. In addition, glacier deformation shows indirect analogies with icy satellite deformation. In fact, the basal friction generated at the glacier/bedrock interface cannot be directly compared with the icy satellite crust, which is composed of the same material. However, deep variations due to phase transitions of the ice or internal discontinuities can occur within their crust, and at a local -scale, they might affect the kinematics of the shear corridors. On the other hand, for instance, ice shelves floating on the ocean cannot be considered for such an approach since they exhibit a different deformation style from the shear zones.

The contribution of terrestrial analogs represents a key resource for understanding remote planetary surfaces, where, so far, in-situ investigations are impossible [45]. Their comparison provides strong support for the limited remote sensing data of the icy satellites. A recent study has successfully shown the analogy between the structural setting of glaciers and that recognized on icy satellite surfaces [46]. Starting with the comparative study of glacier deformation, the authors suggested that the subsurface setting of shear corridors on icy satellites is pivotal for the balance of their tectonics. This deep setting is mainly characterized by diffuse low-angle structures, among which compressional structures, called thrusts, develop. Such structures are crucial for tectonic balance, and in turn, their detection is valuable for planetary geologists to understand how the amount of extension on icy satellites can be compensated. Moreover, the detection of compressional structures contributes to constraining a tectonic model that can be applied to the icy satellite crusts.

In this way, the analogy of the deformation pattern recognized on glaciers allows for a better understanding of the detection of compressional structures, which are difficult to identify on icy satellite surfaces. Glaciers exhibit both local- and regional-scale deformation structures. The knowledge gained from their comparison is then transferred to the study of icy satellites, to better understand their structural settings in strike-slip shear zones.

In this work, we focus on compressional structures in icy environments, whose detection is useful for understanding icy satellite deformation. We provide a review of thrusts known to exist on glaciers, their morphological occurrence, their detection at different investigation scales, and the implications they offer for their possible detection in remote areas of icy satellites.

Methods used for their detection are explained and can be applied to the icy satellite case. Thanks to multiscale analysis combining fieldwork and remote sensing investigation of glaciers, we propose an approach to suggest the occurrence of such compressional structures on icy satellites, which are otherwise difficult to detect with remote sensing alone. This allows us to improve their investigation on these icy bodies. Examples of compressional structures identified in glaciers located in the Greenland Ice Sheet and the Southern Patagonian Icefield are shown. These will be used as models for the icy satellite strike-slip shear zones, helping to better contextualize their structural patterns at the local -scale and understand the location of compressional structures. The examples shown in this work lead to a conceptual model of the surface and subsurface structural pattern of shear zones in icy satellites.

2. Background

Glaciers slide downslope due to gravity [25]. In the upper portions, they thicken by accumulating mass, while the lower part is characterized by deformation and thinning due to the flow under their own weight. In these regions, glaciers primarily deform by exhibiting a complex array of structural features that reflect the dynamic processes [47]. The resulting structures are the outcome of both brittle and ductile deformation mechanisms caused by transversal and longitudinal stresses, and they provide insight into the structural evolution of glaciers and how they deform (Figure 1). Fractures and crevasses are widespread on glaciers and typically form in areas subjected to tensile stress. They develop perpendicular to the direction of the greatest extension (i.e., the minimum principal stress σ^3) and are most commonly found near the glacier's surface, in the upper brittle layer [24,41]. Brittle fractures are identified both at the glacier's center and along its margins. Longitudinal crevasses typically occur at the glacier's center, where the ice stretches along the flow direction, while transverse crevasses form in areas of accelerating flow, such as irregularities in the bedrock topography [19,48,49]. These fractures indicate the stress distribution within the glacier, and their patterns change over time in response to glacier velocity, temperature, and strain rate [50–52]. Their formation is often triggered by surge events, which are short periods of rapid glacier movement during which large stresses and strain rates are reached [53,54]. Consequently, many fractures are remnants of such highly dynamic periods in the glacier's history. Between surge phases, ductile processes dominate, and fractures tend to decrease [25,55].

What we observe at the glacier surface is its permanent deformation, exhibiting both brittle and ductile structures that coexist in cross-section. The occurrence of these deformation structures, according to the glacier's rheology, varies vertically from the brittle surface to the ductile bottom [14,47].

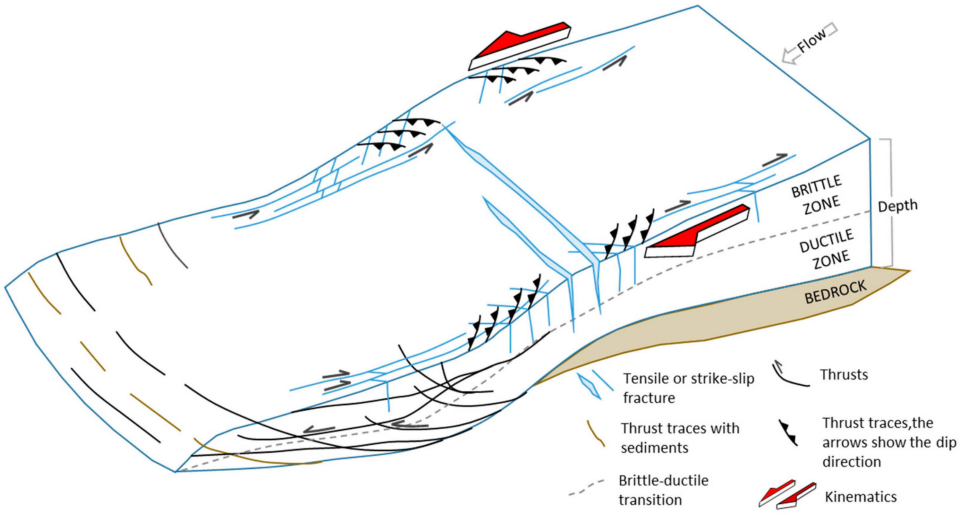


Figure 1. Structural pattern of glacier's profile (modified from [25]).

We observe the permanent deformation formed during the glacier's history, whose structural pattern is consistent with strike-slip and compressional dynamics [19,26,27,56,57]. Shear is prominent in glaciers, especially at their margins, which are most affected by the kinematics of the ice flow, causing friction with the close bedrock [47]. Compressional flow typically occurs at the base of glaciers or near their terminus, where higher-pressure conditions cause the ice to deform plastically and develop folds and thrusts [58]. This regime is primarily associated with surge events in the glacier, during which velocity and strain rate increase [54].

Both of these regimes produce thrusts, and their detection is useful for gaining information about compressional structures on icy satellite regions, which exhibit structural pattern similar to that observed on glaciers (i.e., the shear corridors).

2.1. Strike-Slip

Strike-slip deformation occurs when the maximum and minimum principal stresses (σ^1 and σ^3, respectively) are in the horizontal plane, resulting in the horizontal displacement of two blocks that slide past each other without the creation or convergence of the portions under stress (Figure 2a) [41,43]. Shear zones accommodate lateral flow by undergoing intense deformation, often associated with striations or drag folds. The resulting deformation structures typically exhibit a nearly vertical dip and often crosscut and offset other fractures in accordance with their sense of movement. At the regional -scale, this regime produces wide, elongated zones of shear bordered by long strike-slip structures. These regions experience associated deformation, where a variety of individual elements, ranging from strike-slip to dip-slip extensional and compressional structures, are formed [43]. The kinematics of glaciers is consistent with the shear zones produced by strike-slip (Figure 1). In fact, the glaciers flow and show horizontal displacement at their margins, similar to the strike-slip zones. At the contact with the surrounding bedrock, the glacier moves and deforms similar to a block that has been displaced along the horizontal plane in a strike-slip zone.

Thus, the stress fields that generate extensional and compressional deformation structures recognized within the glacial body are framed within the kinematics of the glacier's downward sliding. As non-homogeneous bodies, the strike-slip activity of glaciers includes a complex array of subsidiary deformation structures, including compressional faults. Thrusts trend at an angle of 45° or less to the main faults that delimit the shear zone boundary, which, in this case, is the glacier's margin. Depending on the extensional

or compressional components associated with the shear, their trending angle varies; it decreases in transpressional regimes and increases in transtensional regimes [43].

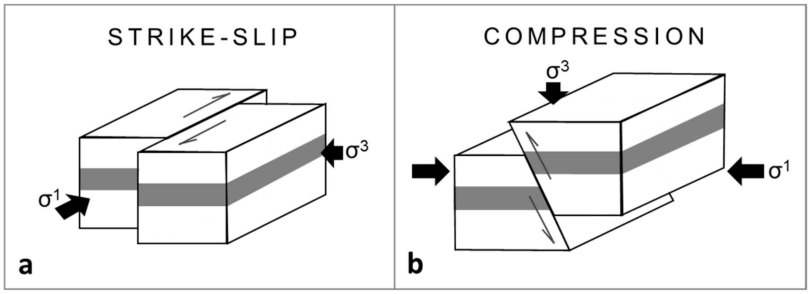


Figure 2. Block models of the (**a**) strike-slip and (**b**) compressional faults, with main stress axis orientation.

2.2. Compression

From certain perspectives, glaciers can also be considered analogs of *fold-and-thrust* tectonic belts or gravitationally driven thrust sheets [25,26]. Compression occurs when the maximum principal stress σ^1 is horizontal (and the minimum principal stress σ^3 is vertically oriented), leading to the shortening and thickening of the portion of the material under stress (Figure 2b; [41]). Although compressive stresses are generated in glaciers dynamics, the conditions for the formation of thrust faults in glaciers remain controversial and are even considered implausible by some [59]. Authors have discussed the feasibility of the mechanical compression process, which cannot always occur given the properties of glacier ice-*Ih* [60]. Ice fracturing under compression depends on the principal stress, the frictional properties and rheology of the ice, and the geometry of the fractures [61]. In addition, the ice's ability to resist stress without undergoing permanent deformation through fracturing or flow, known as strength, plays a key role in the potential development of compressional structures, such as folds and thrusts [62,63].

Polycrystalline ice has a compressive strength that increases with decreasing temperature and increasing strain rate, in contrast to its tensile strength, which decreases as the grain size increases [64]. Like rocks, the ice strength in compression is larger than in extension. The tensile strength varies from 0.7 to 3.1 MPa, while the compressive strength ranges from 5 to 25 MPa, under the same strain rate and temperature (varying from −10 °C to −20 °C) [64].

Theoretically, based on numerical models, thrust faulting can occur during surges in non-homogeneous, thin ice where pre-existing fractures represent structural weaknesses [59]. Therefore, we can expect a smaller number of thrusts on glaciers compared to the recognized tensile fractures at their surfaces. However, a large number of thrusts have been detected on glaciers, as they are non-homogeneous bodies, and structural geology analyses reveal the occurrence of compressional structures [65,66]. Compressive stresses produce structures that vary from ductile folds to brittle thrusts, depending on local conditions such as temperature, velocity and substrate geometry. Thrusts on glaciers are mostly recognized at the localscale and occur through different mechanisms.

2.3. Glacial Thrusts

Although the mechanical processes required to form thrust faulting are difficult to achieve (due to the large strength and strain rates necessary for their development), field structural investigations on outcrops show the viability of compressional structures in glaciers [46,65,66].

Due to gravity, which governs glacial flow, the compressive forces induced by glacier kinematics are generally longitudinal and form structures with a concave-upward shape

that advance in the direction of the kinematics (Figure 3a; [67,68]. These are compressional faults, i.e., thrusts that form orthogonally to the maximum principal stress σ^1, and their movement is accommodated by a dip-slip relationship, usually < 30° (Figure 2b; [41]). They can also be oblique-slip structures due to the contribution of a strike-slip component, which produces a transpressional stress regime [69].

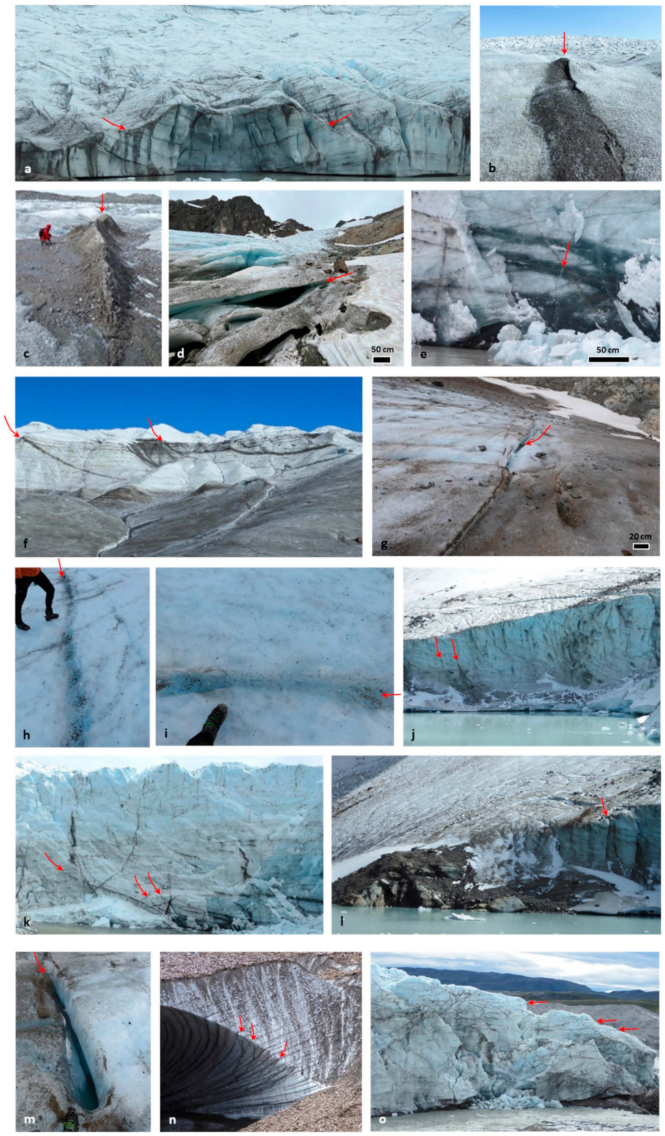


Figure 3. Examples of thrust in glaciers shown by the red arrows in the panels. (**a**) Southern margin of Isunguata Sermia glacier in the Greenland Ice Sheet. The glacier profile shows the thrust concave upwards morphology. Debris band through sediment transportation by thrust activity in (**b**) Isunguata Sermia glacier and in (**c**) Russell glacier in the Greenland Ice Sheet. (**d**) Deep structural network developed within the low-angle thrusts in the Vinciguerra glacier of the Tierra del Fuego region in Argentina and (**e**) fluid migration and leakage from thrusts at the terminus of Russell glacier in the Greenland Ice Sheet. Thrust category I in (**f**) Isunguata Sermia glacier in the Greenland Ice Sheet and in (**g**) the Alvear glacier in the Tierra del Fuego region in Argentina. (**h**,**i**) Thrust category II in the Alvear glacier in the Tierra del Fuego region in Argentina. Thrust category III in (**j**) the terminus of the Ojo del Albino glacier in the Tierra del Fuego region in Argentina and in (**k**) the terminus of Russell glacier in the Greenland ice Sheet. Thrust category IV in (**l**) the terminus of the Ojo del Albino glacier and in (**m**) Alvear glacier in the Tierra del Fuego region in Argentina. Thrust category V in (**n**) the glacial cave Cueva de hielo de la Oveja in the Tierra del Fuego region in Argentina and in (**o**) the terminus of Russell glacier in the Greenland Ice Sheet.

Therefore, thrust-faulting activity is pivotal for glacier sliding and often marks the transition of ice from brittle to ductile behavior [25,70–72]. Thrust movement allows the entrainment of sediments that are taken from the basal bedrock and transported upwards toward the margins and terminus of the glacial body [73–75]. This process is manifested by ice ridges or push moraines, where debris is accumulated and deposited by the glacier's advance (Figure 3b,c; [76,77]). Moreover, being deep sub-horizontal structures, thrusts in glaciers represent significant subsurface networks that act as conduits, allowing debris and fluids to migrate within the icy mass toward the tip of the structures (Figure 3d,e; [78]).

In the field, different factors characterize the occurrence of compressional faults. Here, we present five categories of glacial thrusts recognized at the outcrop scale (Table 1):

(I) Thrusts typically develop with a gentle low-angle dip, which steepens up to 40° as they reach the surface, forming small steps, duplexing the topography (i.e., topographic growth due to the thrust kinematics that leads to internal layer repetition) or cutting the topographic slopes (Figure 3f,g). Usually, thrust traces are darker than the surrounding ice due to the transport of debris from the underlying bedrock, soil and dust.

(II) Together with percolation water, the friction produced by the sliding of the thrust planes causes ice melting and lubrication, which can subsequently refreeze, resulting in the healing of the thrust fracture (Figure 3h,i). In fact, the process of compression, melting, and refreezing, or pressure solution [25,41], eliminates air bubbles from the ice, resulting in a dense, coarse crystalline ice structure [22]. In this way, the linear trace of such thrusts is shown on the surface as clear ice, also referred to as 'blue ice'.

(III) Thrusts can develop by remaining at depth or nearly parallel to the bottom, becoming blind, and not reaching the surface (Figure 3j,k). The latter can be exposed at the surface at a later stage [14].

(IV) In addition, compressional structures often develop on pre-existing weakness planes in the ice, such as fractures and crevasse (Figure 3l,m). This occurs as a result of reactivation of older tensile fractures [51,59]. In this way, these thrusts appear on the surface with a high-angle dip that tends to flatten at depth.

(V) Moreover, at depth, thrusts can often be concealed within the glacier layers, which facilitate their occurrence and motion, similarly to how bedrock thrusts often form on weak lithologies, such as clay, or lithological variations that act as *décollement*, allowing thrust kinematics [41]. Therefore, ice layers within the glacier can also be reactivated as thrusts (Figure 3n,o).

Table 1. Categories of glacial thrusts and their description, morphology and best techniques for detection.

Thrust Category	Description	Surface Traces	Detection Technique
I	Thrusts with low-angle dip < 40° as they reach the surface by forming small steps, duplexing the topography or cutting the topographic slopes.	Darker than the surrounding ice due to the debris entrainment.	Fieldwork Structural mapping Spectral analysis Ground Penetrating Radar
II	Thrust movement produces ice melting and subsequent water freezing by healing of the fracture.	Dense, coarse crystalline and clear ice, also referred to as 'blue ice'.	Fieldwork Structural mapping Spectral analysis
III	Deep thrusts that develop nearly parallel to the bottom without reaching the surface.	No occurrence at surface. Later exposure can occur due to erosion of the glacier surface.	Fieldwork Ground Penetrating Radar

Table 1. *Cont.*

Thrust Category	Description	Surface Traces	Detection Technique
IV	Thrusts that develop on pre-existing fractures and crevasse.	High-angle dip that tends to flatten at depth.	Fieldwork Structural mapping Ground Penetrating Radar
V	Thrusts develop among the glacier layers.	No occurrence at surface. Can be detected on slopes within the ice stratification.	Fieldwork Ground Penetrating Radar

Thrusts crosscut each other, resulting in a complex structural pattern. Nevertheless, recurring relationships are identified at different investigation scales.

2.4. Icy Satellites

The icy satellites show strong evidence of tectonic activity, manifested by kilometer-scale structures that deform the surface of many of them, including, for instance, Europa, Ganymede, Enceladus, Dione, Miranda [28,79]. The tectonic structures recognized at the surface are the result of brittle deformation, mainly produced by extension and strike-slip [34,80,81]. In particular, the surface of the icy satellites is characterized by long strike-slip shear zones that produce a complex tectonic pattern with subsidiary structures identified within such regions (Figure 4; [39]).

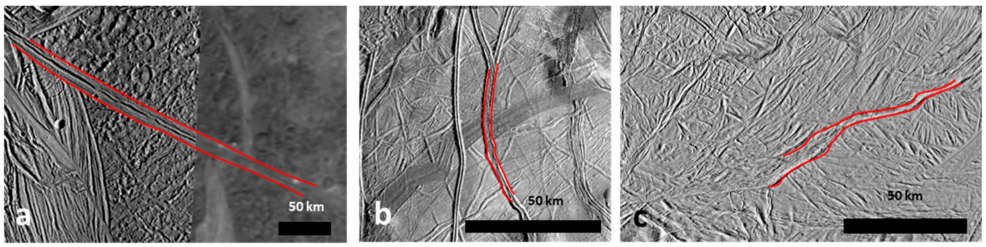


Figure 4. Examples of shear corridors defined by the red lines on icy satellites (**a**) Ganymede, (**b**) Europa and (**c**) Enceladus. The offset of other structures represents kinematic indicators produced by these shear zones.

On Ganymede, deformation structures called grooves are identified on the light grooved terrain (Figure 4a). These structures are linear to curvilinear subparallel ridges and troughs, with lengths greater than 100 km and average spacing of about 10 km, shaping the light terrain [82]. They show a graben-like morphology and are often arranged in a tilt-block-style normal faulting, representing a geometry of normal faults dipping in the same direction [42]. The expression of extension on Ganymede's surface is formed by instabilities in a ductile lithosphere that reshaped preexisting terrain through tectonic resurfacing [83]. Ganymede's light terrain also shows a large number of strike-slip structures that horizontally displace other structures. Examples of shear zones are identified on Uruk Sulcus, Dardanus (centered at 17.5° S, 342.5° E; [84–87]), Arbela Sulcus (21.1° S, 10.2° E; [86,88]), Nun Sulci (49.5° N, 43.6° E; [86,87,89]), Nippur/Philus Sulcus (36.9° N, 175° E), Byblus Sulcus (37.9° N, 160.1° E), Anshar Sulcus (18°N, 162.1° E; [86] and references therein), Tiamat Sulcus (3.4° N, 151.5° E), Kishar Sulcus (6.4° S, 216.6° W; [84,89,90]), and Harpagia Sulcus (11.8° S, 313.5° W; [88,91]).

The surface of Europa was also greatly modified by tectonic activity. Lithospheric separation and spreading strongly show the contribution of the extensional regime on Europa [92,93]. A complex superposition of troughs, ridges, and dilatational bands (i.e., polygonal areas of smoother terrain with sharp boundaries) characterizes its surface [94]. In addition, tensile stress due to diurnal tides formed long chains of arcuate ridges, called cycloids [95]. Europa's surface provides the unique example of pure compression on icy satellites. Indirect evidence suggests the occurrence of folds [96] and subduction-like structures, called subsumption [97]. The latter have been recognized through tectonic restoration of bands and represent one of the first models of a plate tectonic-like system beyond Earth. The tangle of troughs and ridges deforming the surface of Europa also shows a great variety of strike-slip indicators (Figure 4b). Examples show band-like appearances and can be recognized on Astypalaea Linea (75,8° S, 212,1° W), Agave Linea (12,8° N, 273,1° W; [98,99]), Agenor Linea (40.9° S, 186.5° W; [33,100]), Corick Linea (17,8° N 18,3° W; [100,101]) and Katreus Linea (38,8° S, 213,3° W; [100–102]).

Enceladus shows strong deformation in three main regions, called Leading Hemisphere Terrain, Trailing Hemisphere Terrain and South Polar Terrain [103]. These terrains show similarities, as each includes a circumferential belt that encloses one or more other structurally deformed units. The main and most active region is the South Polar Terrain, where four sub-parallel main strike-slip faults, called Tiger Stripes, dominate the region [104]. The area is affected by right-lateral kinematics, and the strike-slip boundaries are located in the Sub-Saturnian Margin (centered at 34°45′ W, 57°19′ S) and in the Anti-Saturnian Margin (centered at 144°27′ E, 53°51′ S; [40]). The other two terrains show similar geometries and structures, suggesting the relict location of old polar terrain [105]. Shear corridors characterize these areas (Figure 4c).

Table 2 shows the main characteristics of these three icy satellites. Although oblique tectonics have been identified with a compression through transpressional regime (e.g., [44]), few compressional structures have been identified at the brittle surface of tectonized icy satellites. This paucity represents an open question concerning the tectonic compensation of the total amount of extension and strike-slip recognized at the surface.

Similar to glaciers, the brittle surface of the icy satellites is replaced at depth by ductile behavior after a transition zone, usually lying kilometers beneath the surface (e.g., Ganymede < 10 km, Europa < 3 km [34,106]). As a result, their structural pattern changes vertically with the rheological variation of the crust. Moreover, the stronger ice strength in compression also applies to these icy bodies (e.g., Ganymede's lithosphere is ~3 times stronger [107]). This assumption makes the occurrence of compressional structures on the crusts of the icy satellites more difficult.

Nevertheless, the crust of the icy satellites can be heterogeneous, i.e., an ice mixture with silicate dust (e.g., [108]). This implies that compression can occur on icy satellite crusts and can be reached in strike-slip zones. In this way, indirect considerations can be inferred from what is observed on glaciers.

Therefore, the detection of compressional structures is pivotal for understanding the dynamics that affect the icy satellites and their geological and tectonic evolution. Moreover, it allows us to make inferences about the structural network that develops at depth, helping us gain knowledge about the deformed volume of their upper crust and the implications for fluid propagation at depth. Figure 5 shows the potential structure network that can develop below the surface of shear corridors on icy satellites. According to what has been learned from glaciers, the upper crust of the icy satellite shear zones can show a similar structural pattern, including low-angle thrusts developing at depth.

Table 2. Characteristics of the icy satellite's interior, tectonic structures and relative morphology.

Icy Satellites	Description	Tectonic Structures	Surface Traces
Ganymede	Jupiter's largest satellite, composed by an icy crust, a liquid water ocean, a HP ice mantle and a metallic core.	Grooves and furrows, formed by extensional and strike-slip	Regional-scale linear to curvilinear kilometer-long traces that crosscut and intersect each other. Grooves occur in the youngest light terrain.
Europa	Jupiter's satellite, composed by an icy crust, a water ocean, a rocky mantle and a metallic core.	Troughs, ridges, bands and cycloids that shape the surface by extensional and strike-slip regimes. Folds and subduction-like evidence have been interpreted.	Regional-scale linear to curvilinear kilometer-long traces that crosscut and intersect each other in most portions of the surface.
Enceladus	Saturn's satellite, composed by an icy crust, a water ocean and a rocky core.	Active body with plume eruption from Tiger Stripes faults at the South Pole, formed by strike-slip regime.	Regional-scale linear to curvilinear kilometer-long traces that crosscut and intersect each other, mostly in the southern terrains.

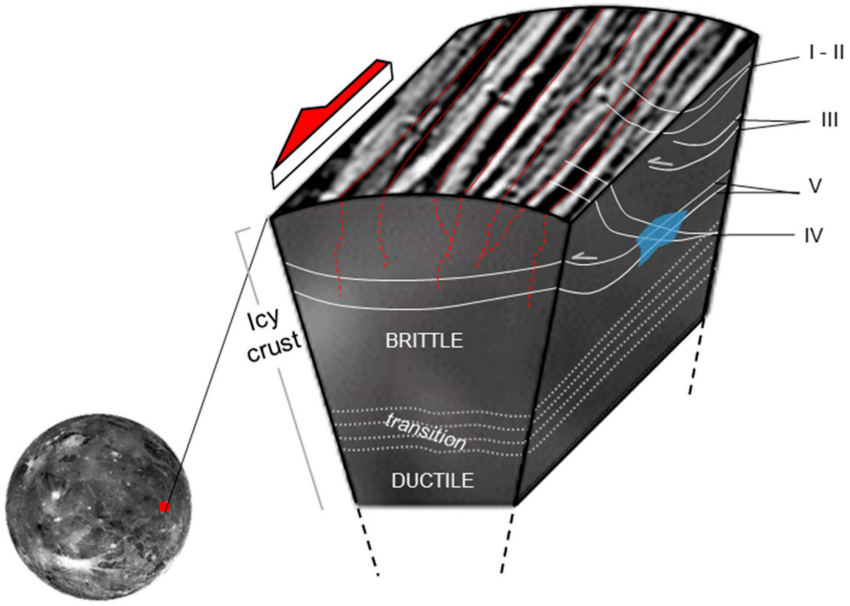


Figure 5. Conceptual model of the surface and subsurface structural pattern on shear zones of icy satellites. The red lines show the extensional and strike-slip structures and their development at depth (dashed red lines). The grey lines show the occurrence of deep thrusts subdivided into categories I–V and their possible orientation at surface. The deep thrust network can originate from a fluid reservoir, shown by the light blue feature. The red arrow shows the sense of movement of the corridor.

3. Approaches and Examples

The methodology used to detect compressional structures on icy satellites is broad. In particular, glaciers and icy satellites share similarities that can be compared through multiscale analysis. The same ice-*Ih* material and the same deformation styles that affect shear zones are observed on both bodies at a variety of scales. A multiscale approach is crucial to corroborate findings obtained through remote sensing at the regional scale and to make predictions about local-scale environments of icy satellite surfaces. In this way, satellite imagery must be compared with ground observations. Fieldwork is the main

technique used to collect data at the outcrop scale. This local-scale dataset is then compared with a regional-scale dataset, comprising remote sensing, whose multiple techniques range from optical to spectral analysis and Ground Penetrating Radar (GPR, or ice penetrating radar) investigation. The knowledge acquired from the comparison of these datasets is then applied to the remote sensing data of icy satellites to infer the occurrence of compressional structures in regions deformed similarly to glaciers. Table 3 shows the main methodologies used to perform multiscale analysis between glaciers and icy satellites.

Table 3. Description of the methods and data for the detection of glacial thrusts.

Methods	Description	Data Acquisition	Thrust Detection
Fieldwork	Structural geology techniques for field survey aim at collecting local-scale measures, such as azimuth, length, width, spacing among structures, throw, spatial distribution and crosscutting relationship. Unmanned aerial vehicles (UAVs) or drones support the investigation of remote areas of the glaciers that are unreachable	Structure attributes values at local-scale and represented by rose diagram and stereoplot. Ortho-rectified maps and digital elevation models (DEMs).	Thrusts categories I–V
Structural Mapping	To identify, classify and statistically quantify the structures and their attributes at regional-scale.	Structure attributes values at regional-scale and represented by rose diagram and stereoplot. Structural maps in Geographic Information Systems (GIS) showing the deformation pattern at regional-scale.	Thrusts categories I–II and IV
Spectral analysis	Due to debris entrainment and ice melting, the spectral characteristics of thrust traces at surface are different than the surrounding ice and can be detected by spectral analysis	Spectral data Spectral signature	Thrusts categories I–II
Ground Penetrating Radar	To detect the deep structures and their pattern. Dip and subsurface structure development can be investigated.	Radagrams Crossection profiles	Thrusts categories I-V

3.1. Fieldwork

Structural geology techniques for field survey aim to collect measurements of the deformation structures identified at the local-scale. In particular, the structure attributes are quantified, such as azimuth, length, width, spacing between structures, throw, spatial distribution and crosscutting relationships (Figure 6 [46,65]). These provide key information for unravelling the stress field that affected the study areas [41]. The azimuth refers to the orientation and dip of a structure relative to north, while the slip refers to the relative movement on either side of the fault plane. The spacing between structures with similar orientation allows for the quantification of the fracturing intensity of the ice. The throw indicates the motion of the fault, i.e., the vertical component of the dip separation. Spatial distribution characterizes the possible patterns that provide insights into structure clustering and spatial relationships among elements of a cluster, which are essential for analyzing crosscutting relationships. These crosscutting relationships show the intersection

or mutual interruption of structures, indicating a relative chronology of the deformation to be established.

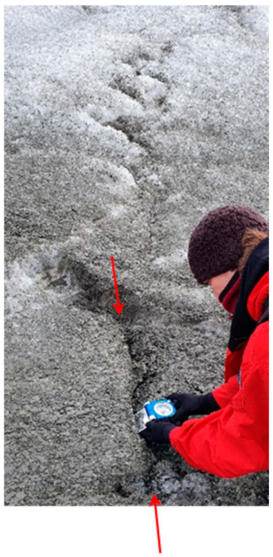


Figure 6. Azimuth measurement of the thrust (shown by the red arrows) with compass clinometer during fieldwork in the Isunguata Sermia glacier in the Greenland Ice Sheet.

Such attributes are measured using field geology instrumentation and are used to perform geostatistical analyses of their frequency distribution.

During fieldwork, the use of unmanned aerial vehicles (UAVs) or drones supports the investigation of remote areas of glaciers that are otherwise unreachable [109,110]. The data obtained by drone survey allow for the creation of ortho-rectified maps and digital elevation models (DEMs), which are used to analyze and interpret the deformation structures using digital outcrop modeling tools [111]. UAV datasets allow for a better comparison with regional-scale satellite images acquired through remote sensing.

3.2. Remote Sensing

Remote sensing techniques are powerful tools for analyzing deformation structures in planetary crusts. Both brittle and ductile structures are commonly observed on the ice surface as relict or inherited features. Mapping these structures and determining their interrelationships is essential for understanding how they respond to stress conditions, providing insights into the long-term dynamic history of the investigated area. Regional-scale investigations are conducted using remote sensing techniques, such as structural mapping, spectral analysis and GPR analyses.

3.2.1. Structural Mapping

Detailed structural mapping is performed to identify, classify and statistically quantify the recognized structures at the regional-scale in areas that cover the investigated field sites [46]. On satellite images and aerial photos, if available, mapping is performed at scales up to 1:5000 to achieve an optimal regional context of the glaciers (Figure 7a,b). On the other hand, the largest scale that can be reached for optimal structural mapping on icy satellites is typically 1:200,000, depending on the image data and the studied body (Figure 7c,d). Deformation structures are identified through both manual and automatic mapping (e.g., [39]). Manual detection is often the first approach used, which helps train a machine learning tool to automatically map the study area. Computer vision tasks (e.g., image classification, object detection, semantic segmentation and instance segmentation) are provided by automated mapping tools based on deep learning networks, such as the convolutional neural

network model of [112], which can detect, classify and map linear surface features. Manual and automatic mapping can also be compared and integrated to avoid biases from either the human operator or the tool. On glaciers, deformation structures with length longer than 10 m are mapped and digitized as polylines in a Geographic Information System (GIS). On icy satellites, structures ranging from hundreds of meters to several kilometers in length are mapped. Morphological indicators help to unravel the structure kinematics, such as possible dip-slip or strike-slip relationships of the mapped structures. In addition, the digitized structures are measured to obtain their attributes, which are then quantified through statistical analyses.

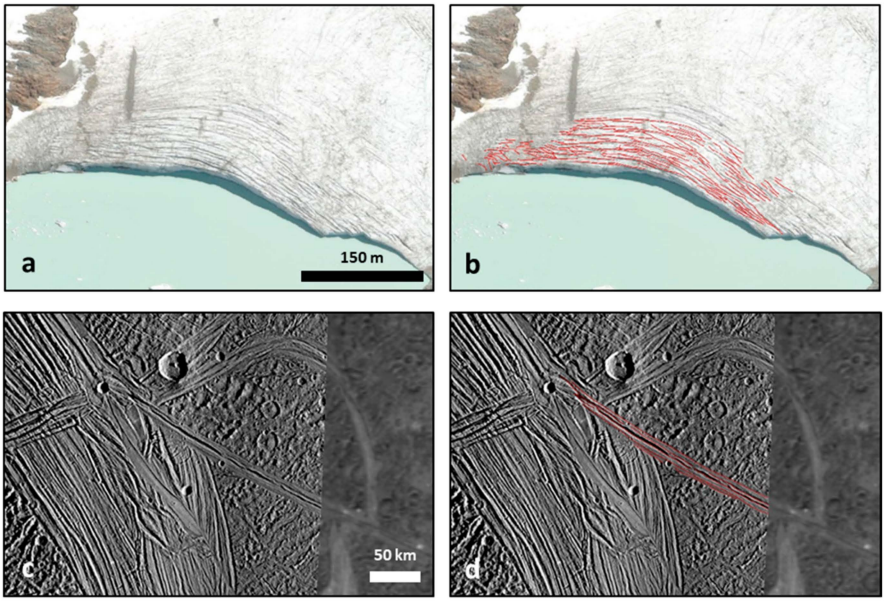


Figure 7. Examples of structural mapping in (**a**,**b**) Ojo del Albino glacier (Maxar high-resolution images) and in (**c**,**d**) Tiamat Sulcus, Ganymede (Voyager and Galileo Global mosaic [113]). The mapped structures are shown in the right panels in red color.

For regional-scale detection of glacier thrusts belonging to categories I and II, their faint traces, which are often darker because they are filled with sediments or contain fluids, can usually be detected. Thrusts of category IV are easier to detect, though they may be mistakenly interpreted as extensional structures. Thrusts of categories III and V cannot be mapped because they do not reach the surface.

3.2.2. Spectral Analysis

Since thrusts often entrain debris or can be wetted by melted ice, their traces on the surface may appear darker or different from the surrounding ice. Often, these traces are healed by clear ice, which refreezes due to frictional melting caused by the thrust motion (thrusts of category II). Consequently, recurrent, long and thin linear traces composed of different materials absorb and reflect light differently (Figure 8 [114,115]). Their spectral characteristics, which differ from the surrounding ice, can indicate the presence of thrusts. This assumption is placed within the context of the deformation recognized in the study area.

Therefore, spectral analysis allows us to detect the thrust impurities composed of the transported material and to quantify the different behavior of the clear ice, particularly in the visible and near-infrared range [115]. This represents another valuable method for detecting the possible occurrence of compressional structures on high-resolution satellite images.

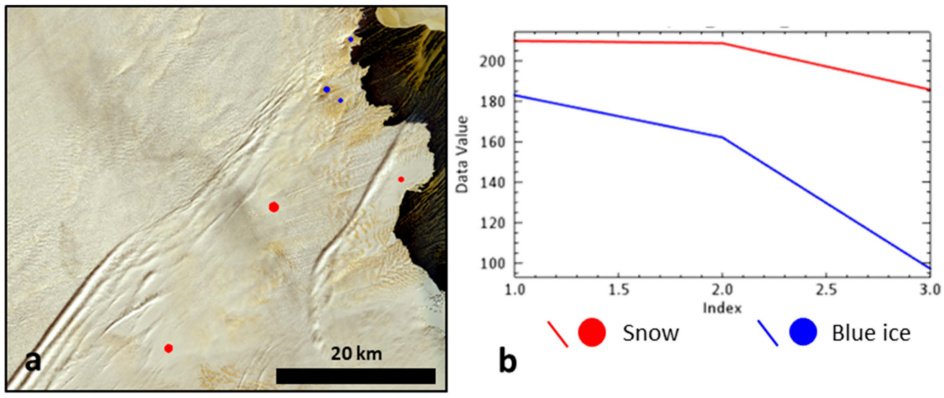


Figure 8. Example of spectral analysis in (**a**) false color image (G, B, NIR) of a portion of the ice sheet Preston Heath in Wilkes Land (Antarctica) where patches of blue ice areas are evidenced in light yellow color. Circles of regions of interest show the different outcropping ice (red points show snow areas, while blue points show blue ice) used to analyze the (**b**) spectral signature.

On the icy satellites, spectral analysis can reveal differences in surface composition, which may be evidence of deformation structures whose activity dislodges the crustal components.

This method allows us to detect thrusts of category I and II on the surface, which may exhibit traces with varying amounts of dust or other components, such as volatiles trapped in clathrate hydrates, in comparison with the surrounding surface.

3.2.3. Ground Penetrating Radar

GPR is a useful remote sensing technique that uses radar pulses to image the subsurface [116,117]. The acquired data allow us to detect the deep pattern followed by ice features. Profiles of the internal architecture of the ice mass provide insights into its thickness, stratigraphy and dynamics. In fact, the development of deformation structures can also be investigated. Fractures can be detected because radar waves reflect off the boundaries between the voids of the crevasse and the surrounding ice. GPR analysis can also detect concealed structures, such as snow-covered fractures or blind thrusts (category III).

In particular, because they contain discontinuities, thrusts generate strong reflections of the signal and appear as anomalies or interruptions of the normal pattern of the internal ice layering (Figure 9; [65,72,75,116]). Thrusts are usually more inclined or cut through the sub horizontal ice layers. Their geometry is often concave-upward and can produce a more intense reflection plane, as the presence of debris or clear ice contrasts with the surrounding ice. This contrast can occur when the ice melts within the thrust, causing a change in reflectivity between ice and water. Signal difference can also be detected due to the complexity of the thrust shape, which deforms the ice in different directions, in turn causing chaotic variations in reflection angles. This is then observed in radargrams that show a confused pattern compared to the regular layering.

Therefore, GPR allows us to detect thrusts by unraveling their development from surface to depth (category I and II) and even confirming their effective nature (category IV). Moreover, such analysis enables the detection of thrusts that do not reach the surface (category III and V).

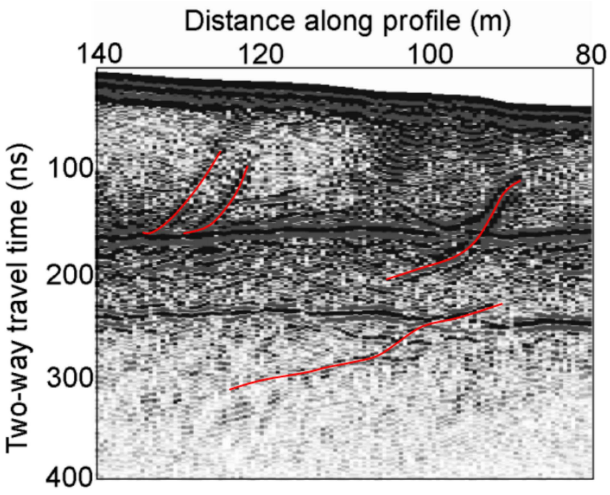


Figure 9. Example of G profile of Kongsvegen glacier, Svalbard. The red lines show the occurrence of deep thrusts (modified from [116]).

4. Discussion and Summary

Compressional structures, known as thrusts, have not yet been identified on icy satellites. However, structural investigations of their surfaces suggest the presence of such features, despite their absence in remote sensing data. The analogy between the glacial deformation style and that observed on shear zones of several icy satellites allows us to compare their structural patterns and make inferences about the potential occurrence of thrusts in such remote environments.

On glaciers, thrusts play a fundamental role in understanding how compression develops, providing insights into the deformation occurring on icy satellites. Our review of compressional structures in terrestrial icy environments aims to improve the understanding of their detection on remote surfaces, where remote sensing is the main tool available. The correlation between glacier dynamics and icy satellite shear zones helps address the broader question of tectonics on icy satellites, using the knowledge gained from the study of terrestrial ice masses.

Thrusts, even on Earth, are difficult to detect using remote sensing due to their subtle morphological characteristics. They are often challenging to map at the regional-scale because of their low-angle dip and the minimal stratigraphic repetition they produce. Local-scale analyses, however, reveal their locations, orientations, and subsurface development. By employing a multiscale approach, we can make inferences about their occurrence on icy satellites, particularly in the shear zones that characterize these surfaces.

This challenge highlights the need for a multifaceted approach, combining remote sensing with detailed structural measurements from field studies. Local-scale analysis of glaciers, for example, provides valuable insights into how icy masses deform under stress, which can be applied to the study of icy satellites. In addition, the proposed methods represent a strong tool that can help us detect compressional structures.

In this work, we highlight the morphology of the thrusts and the implications their occurrence may have for icy satellite crusts. The significance of detecting potential thrusts allows us to understand the tectonic models applied for icy crusts and to explore the development of the internal fracture network composed of both high- and low-angle structures, which may serve as internal conduits for liquid propagation. In addition, the detection of compressional structures could indicate the presence of internal reservoirs enclosed by folds. Figure 5 shows the schematic model of the structural pattern of a shear zone recognized on icy satellites (Ganymede is used as an example). This model illustrates a portion of the icy crust, from the brittle top to the ductile depth, affected by left-lateral

deformation. Long and sub-parallel structures detected at the regional-scale deform the surface of this zone (red lines). These are mostly strike-slip faults whose development at depth is interpreted as nearly vertical (dashed red lines), penetrating the brittle crust. At depth, low-angle structures are assumed to exist within the brittle portion of the crust (light grey lines). These are thrusts that can reach the ductile crust, suggesting a wide transition zone from brittle to ductile. The five categories of thrusts (I–V) develop at depth and can reach the surface, where they are mostly detected at local-scale, with an angle of 45° or less to the shear zone.

The structural pattern at depth shows a complex variety of high- and low-angle structures, whose intersection potentially allows the formation of liquid reservoirs (light blue feature).

Therefore, the presented model and the examples discussed in this work allow us to make inferences about the disrupted environment of icy satellites.

(i) The main categories of thrusts that we investigated at the glacier's surface provide a starting point for understanding what we can expect at the surface of icy satellites. Moreover, this classification provides us the means to detect these structures on icy satellites. On the icy satellites, thrusts of category I can be detected along the margins of the shear zones, where they trend $\leq 45°$ to the shear zone boundaries or are perpendicular to extensional structures. Thrusts I and II can also show traces that may provide evidence of linear features composed of different materials, such as ice mixtures with dust or clear ice, which could support their identification. Detection of these two categories is possible through optical and spectral remote sensing at high resolution, which are onboard on the upcoming missions (JANUS, up to 2.4 m/pixel, and MAJIS, 0.5–5.5 μm, on JUICE [118]; EIS, up to 0.5 m/pixel, and MISE, 0.8–5.0 μm, on Europa Clipper [119]). Thrusts of category IV can be detected through detailed structural analysis of the study area, where high-angle structures are consistent with the occurrence of compression within the shear zone. This category can be revealed along the margins of the shear zone, and, with optical data, penetrating radar data will be crucial. Such instruments will be extremely important for detecting thrust development at depth and, in particular, for investigating categories III and V, which are concealed at depth. At present, no such data are available for icy satellite surfaces. However, penetrating radars are part of the equipment on JUICE and Europa Clipper (RIME, up to a depth of 9 km, and REASON, $\geq$30 km, respectively [120,121].

(ii) A significant amount of brittle deformation, including tensile and strike-slip faults, is observed in the upper portions of icy satellite crusts. These brittle portions cover underlying blind thrusts, which could compensate for the deformation observed at the surface. As such, it is reasonable to hypothesize the presence of deep compressional deformation structures on icy satellites. Thrusts on glaciers typically form at depth, near the brittle–ductile transition zone. Similarly, compressional structures on icy satellites may develop at depth, particularly in regions affected by strike-slip kinematics, which can induce longitudinal compression. Although the location of the brittle–ductile transition on icy satellites varies depending on the body's crust, a large transition zone is assumed, capable of hosting long thrusts that accommodate surface deformation.

(iii) Besides the different deformation processes, a key difference between glaciers and icy satellites is that glaciers are unconfined masses, while the icy satellite crusts are confined bodies. Glaciers are less constrained in balancing their deformation compared to the more constrained deformation of icy satellite shear zones. Nevertheless, the analogies between glaciers and deformed icy satellite surfaces help us understand how observed deformations might be accommodated. In addition, the presence of

thrusts that allow the compensation of unconfined masses, such as glaciers, further supports the assumption of their occurrence on confined bodies, such as icy satellite crusts, which require necessary balancing.

(iv) Thrust motion can generate ice melting on glaciers and create favorable discontinuities for groundwater flow. On icy satellites, compressional structures can similarly serve as conduits for fluid propagation and play a key role in the deep fracture network that could feed potential subsurface liquid reservoirs. These may be sandwiched between crustal layers and occur beneath the ocean that characterizes several icy satellites.

In this way, studying the analogies between glacial thrusts and potential structures on icy satellites allows us to predict where these features might be found in shear zones and prepares us for future observations. Pivotal inferences are advanced, aiding in the exploration of icy satellites.

ESA's JUICE and NASA's Europa Clipper missions will likely provide the necessary data to detect these structures and assess their importance both at the surface and subsurface. This includes potential connections between thrusts, ice layering, different ice rheologies, and possible deep reservoirs. In particular, the search for signs of compressional features could shed new light on the geodynamics of icy satellites, potentially revealing how these satellites evolve over time.

The data collected from glaciers in Greenland and Tierra del Fuego, combined with multiscale comparison, provide a successful approach for studying the remote surfaces of icy satellites and understanding the candidate areas and features to investigate.

Author Contributions: Conceptualization, C.R. and R.P.; Investigation, C.R., R.P., M.M. and E.F.; software, C.R. and R.P.; writing—original draft preparation, C.R.; writing—review and editing, R.P., M.M., E.F., A.L., M.P., L.P., G.M., F.T. and J.B.; project administration, C.R.; funding acquisition, C.R., A.L. and M.P. All authors have read and agreed to the published version of the manuscript.

Funding: This work is part of the UPSIDES and EVIDENCE projects that have received funding from the European Union's Horizon 2020 research and innovation programme under grant agreement No 871149. We gratefully acknowledge funding from INAF through the Mini Grant DISCOVERIES (cup: C93C23008560001). The activity has been realized under the ASI-INAF contract 2023-6-HH.0.

Institutional Review Board Statement: Not applicable.

Informed Consent Statement: Not applicable.

Data Availability Statement: The data presented in this study are available on request from the corresponding author.

Acknowledgments: We acknowledge the insightful comments of J. van Loon and an anonymous reviewer that helped to improve the manuscript.

Conflicts of Interest: The authors declare no conflicts of interest.

References

1. Prockter, L.M. Ice in the solar system. *Johns Hopkins APL Tech. Dig.* **2005**, *26*, 175–188.
2. Bartels-Rausch, T.; Bergeron, V.; Cartwright, J.H.; Escribano, R.; Finney, J.L.; Grothe, H.; Gutiérrez, P.J.; Haapala, J.; Kuhs, W.F.; Pettersson, J.B.C.; et al. Ice structures, patterns, and processes: A view across the icefields. *Rev. Mod. Phys.* **2012**, *84*, 885–944. [CrossRef]
3. Murray, B.J.; Knopf, D.A.; Bertram, A.K. The formation of cubic ice under conditions relevant to Earth's atmosphere. *Nature* **2005**, *434*, 202–205. [CrossRef] [PubMed]
4. Schubert, G.; Spohn, T.; Reynolds, R.T. Thermal histories, compositions and internal structures of the moons of the solar system. In *Satellites*; Burns, J.A., Matthews, M.S., Eds.; Arizona University Press: Tucson, AZ, USA, 1986; pp. 224–292.
5. Hussmann, H.; Sotin, C.; Lunine, J.I. Interiors and evolution of icy satellites. In *Treatise on Geophysics*; Spohn, T., Schubert, G., Eds.; Elsevier: Oxford, UK, 2007; Volume 10, pp. 509–539.

6. Hobbs, P.V. *Ice Physics*; OUP Oxford: Oxford, UK, 2010.
7. Sloan, E.D., Jr.; Koh, C.A. *Clathrate Hydrates of Natural Gases*; CRC Press: Boca Raton, FL, USA, 2007.
8. Finney, J.L.; Bowron, D.T.; Soper, A.K.; Loerting, T.; Mayer, E.; Hallbrucker, A. Structure of a new dense amorphous ice. *Phys. Rev. Lett.* **2002**, *89*, 205503. [CrossRef]
9. Nimmo, F. Icy satellites: Interior structure, dynamics, and evolution. In *Oxford Research Encyclopedia of Planetary Science*; Oxford University Press: Oxford, UK, 2018.
10. Sotin, C.; Tobie, G. Internal structure and dynamics of the large icy satellites. *Comptes Rendus Phys.* **2004**, *5*, 769–780. [CrossRef]
11. Klinger, J. A possible resurfacing mechanism for icy satellites. *Nature* **1982**, *299*, 41. [CrossRef]
12. Hansen, G.B.; McCord, T.B. Amorphous and crystalline ice on the Galilean satellites: A balance between thermal and radiolytic processes. *JGR Planets* **2004**, *109*, E01012. [CrossRef]
13. Sotin, C.; Grasset, O.; Beauchesne, S. Thermodynamical properties of high pressure ices: Implications for the dynamics and internal structure of large icy satellites. In *Solar System Ices*; Schmitt, B., de Bergh, C., Festou, M., Eds.; Springer Science & Business Media: Berlin, Germany, 1998; pp. 79–96.
14. Hambrey, M.J.; Lawson, W. Structural styles and deformation fields in glaciers: A review. In *Deformation of Glacial Materials*; Maltman, A.J., Hubbard, B., Hambrey, M.J., Eds.; Geological Society of London: London, UK, 2000; Volume 176, pp. 59–83. [CrossRef]
15. Montagnat, M.; Castelnau, O.; Bons, P.D.; Faria, S.H.; Gagliardini, O.; Gillet-Chaulet, F. Multiscale modeling of ice deformation behavior. *J. Struct. Geol.* **2014**, *61*, 78–108. [CrossRef]
16. Glen, J.W. Experiments on the deformation of ice. *J. Glaciol.* **1952**, *2*, 111–114. [CrossRef]
17. Barnes, P.; Tabor, D.; Walker, J.C.F. The friction and creep of polycrystalline ice. *Proc. R. Soc. Lond. Ser. A Math. Phys. Sci.* **1971**, *324*, 127–155.
18. Hall, A.M.; Glasser, N.F. Reconstructing the basal thermal regime of an ice stream in a landscape of selective linear erosion: Glen Avon, Cairngorm Mountains, Scotland. *Boreas* **2003**, *32*, 191–207. [CrossRef]
19. Cuffey, K.M.; Paterson, W.S.B. *The Physics of Glaciers*; Academic Press: New York, NY, USA, 2010.
20. Behn, M.D.; Goldsby, D.L.; Hirth, G. The role of grain size evolution in the rheology of ice: Implications for reconciling laboratory creep data and the Glen flow law. *Cryosphere* **2021**, *15*, 4589–4605. [CrossRef]
21. Knipe, R.J. Deformation mechanisms: Recognition from natural tectonites. *J. Struct. Geol.* **1989**, *11*, 127–146. [CrossRef]
22. Colgan, W.; Rajaram, H.; Abdalati, W.; McCutchan, C.; Mottram, R.; Moussavi, M.S.; Grigsby, S. Glacier crevasses: Observations, models, and mass balance implications. *Rev. Geop.* **2016**, *54*, 119–161. [CrossRef]
23. Kellerer-Pirklbauer, A.; Kulmer, B. The evolution of brittle and ductile structures at the surface of a partly debris-covered, rapidly thinning and slowly moving glacier in 1998–2012 (Pasterze Glacier, Austria). *Earth Surf. Proc. Land.* **2019**, *44*, 1034–1049. [CrossRef]
24. Karato, S.I. *Deformation of Earth Materials: An Introduction to the Rheology of Solid Earth*; Cambridge University Press: Cambridge, UK, 2008; p. 463.
25. Jennings, S.J.; Hambrey, M.J. Structures and deformation in glaciers and ice sheets. *Rev. Geoph.* **2021**, *59*, e2021RG000743. [CrossRef]
26. Elliot, D. The motion of thrust sheets. *J. Geophys. Res.* **1976**, *81*, 949–963. [CrossRef]
27. Hudleston, P.J. Structures and fabrics in glacial ice: A review. *J. Struct. Geol.* **2015**, *81*, 1–27. [CrossRef]
28. Murchie, S.L. The tectonics of icy satellites. *Adv. Space Res.* **1990**, *10*, 173–182. [CrossRef]
29. Kattenhorn, S.A.; Hurford, T. Tectonics of Europa. In *Europa*; Pappalardo, R.T., McKinnon, W.B., Khurana, K.K., Eds.; The University of Arizona Press: Tucson, AZ, USA, 2009; pp. 199–236.
30. Bianchi, R.; Casacchia, R.; Lanciano, P.; Pozio, S.; Strom, R.G. Tectonic framework of grooved terrain on Ganymede. *Icarus* **1986**, *67*, 237–250. [CrossRef]
31. Kargel, J.S.; Pozio, S. The volcanic and tectonic history of Enceladus. *Icarus* **1996**, *119*, 385–404. [CrossRef]
32. Moore, J.M. The tectonic and volcanic history of Dione. *Icarus* **1984**, *59*, 205–220. [CrossRef]
33. Prockter, L.M.; Pappalardo, R.T.; Head, J.W., III. Strike-slip duplexing on Jupiter's icy moon Europa. *JGR Planets* **2000**, *105*, 9483–9488. [CrossRef]
34. Nimmo, F. Dynamics of rifting and modes of extension on icy satellites. *JGR Planets* **2004**, *109*, E01003. [CrossRef]
35. Jaumann, R.; Clark, R.N.; Nimmo, F.; Hendrix, A.R.; Buratti, B.J.; Denk, T.; Moore, J.M.; Schenk, P.M.; Ostro, S.J.; Srama, R. Icy satellites: Geological evolution and surface processes. In *Saturn from Cassini-Huygens*; Dougherty, M., Esposito, L., Eds.; Springer: Berlin/Heidelberg, Germany, 2009; pp. 637–681.
36. Martin, E.S. The distribution and characterization of strike-slip faults on Enceladus. *Geoph. Res. Lett.* **2016**, *43*, 2456–2464. [CrossRef]
37. Yin, A.; Pappalardo, R.T. Gravitational spreading, bookshelf faulting, and tectonic evolution of the South Polar Terrain of Saturn's moon Enceladus. *Icarus* **2015**, *260*, 409–439. [CrossRef]

38. Pizzi, A.; Di Domenica, A.; Komatsu, G.; Cofano, A.; Mitri, G.; Bruzzone, L. Spreading vs. rifting as modes of extensional tectonics on the globally expanded Ganymede. *Icarus* **2017**, *288*, 148–159. [CrossRef]
39. Rossi, C.; Cianfarra, P.; Salvini, F. Structural geology of Ganymede regional groove systems (60° N–60° S). *J. Maps* **2020**, *16*, 6–16. [CrossRef]
40. Rossi, C.; Cianfarra, P.; Salvini, F.; Bourgeois, O.; Tobie, G. Tectonics of Enceladus' south Pole: Block rotation of the tiger stripes. *JGR Planets* **2020**, *125*, e2020JE006471. [CrossRef]
41. Fossen, H. *Structural Geology*; Cambridge University Press: Cambridge, UK, 2010.
42. Pappalardo, R.T.; Head, J.W.; Collins, G.C.; Kirk, R.L.; Neukum, G.; Oberst, J.; Giese, B.; Greeley, R.; Chapman, C.R.; Helfenstein, P.; et al. Grooved terrain on Ganymede: First results from Galileo high-resolution imaging. *Icarus* **1998**, *135*, 276–302. [CrossRef]
43. Fossen, H.; Cavalcante, G.C.G. Shear zones—A review. *Earth Sci. Rev.* **2017**, *171*, 434–455. [CrossRef]
44. Rossi, C.; Cianfarra, P.; Salvini, F.; Mitri, G.; Massé, M. Evidence of transpressional tectonics on the Uruk Sulcus region, Ganymede. *Tectonophysics* **2018**, *749*, 72–87. [CrossRef]
45. Baker, V.R. Terrestrial analogs, planetary geology, and the nature of geological reasoning. *Planet. Space Sci.* **2014**, *95*, 5–10. [CrossRef]
46. Rossi, C.; Cianfarra, P.; Lucchetti, A.; Pozzobon, R.; Penasa, L.; Munaretto, G.; Pajola, M. Deformation patterns of icy satellite crusts: Insights for tectonic balancing and fluid migration through structural analysis of terrestrial analogues. *Icarus* **2023**, *404*, 115668. [CrossRef]
47. Greve, R.; Blatter, H. *Dynamics of Ice Sheets and Glaciers*; Springer Science & Business Media: Berlin/Heidelberg, Germany, 2009.
48. Meier, M.F. *Mode of Flow of Saskatchewan Glacier, Alberta, Canada*; US Government Printing Office: Washington, DC, USA, 1960; p. 351.
49. Benn, D.I.; Evans, D.J.A. *Glaciers and Glaciation*; Hodder Education: London, UK, 2010.
50. Nye, J.F. A method of determining the strain-rate tensor at the surface of a glacier. *J. Glaciol.* **1959**, *3*, 409–419. [CrossRef]
51. Hambrey, M.J.; Müller, F. Structures and ice deformation in the White Glacier, Axel Heiberg Island, North West Territories, Canada. *J. Glaciol.* **1978**, *20*, 41–66. [CrossRef]
52. Campbell, S.; Roy, S.; Kreutz, K.; Arcone, S.A.; Osterberg, E.C.; Koons, P. Strain-rate estimates for crevasse formation at an alpine ice divide: Mount Hunter, Alaska. *Ann. Glaciol.* **2013**, *54*, 200–208. [CrossRef]
53. Lawson, W.J.; Sharp, M.J.; Hambrey, M.J. The structural geology of a surge-type glacier. *J. Struct. Geol.* **1994**, *16*, 1447–1462. [CrossRef]
54. Lovell, H.; Fleming, E.J. Structural evolution during a surge in the Paulabreen glacier system, Svalbard. *J. Glaciol.* **2023**, *69*, 141–152. [CrossRef]
55. Mayer, H.; Herzfeld, U.C. Structural glaciology of the fast-moving Jakobshavn Isbræ, Greenland, compared to the surging Bering Glacier, Alaska, USA. *Ann. Glaciol.* **2000**, *30*, 243–249. [CrossRef]
56. Kehle, R.O. Deformation of the Ross ice shelf, Antarctica. *Geol. Soc. Am. Bull.* **1964**, *75*, 259–286. [CrossRef]
57. Phillips, E.; Everest, J.; Evans, D.J.A.; Finlayson, A.; Ewertowski, M.; Guild, A.; Jones, L. Concentrated, "pulsed" axial glacier flow: Structural glaciological evidence from Kvíárjökull in SE Iceland. *Earth Surf. Proc. Land.* **2017**, *42*, 1901–1922. [CrossRef]
58. Hudleston, P.J. Similar folds, recumbent folds, and gravity tectonics in ice and rocks. *J. Geol.* **1977**, *85*, 113–122. [CrossRef]
59. Moore, P.L.; Iverson, N.R.; Cohen, D. Conditions for thrust faulting in a glacier. *J. Geophys. Res.* **2010**, *115*, F02005. [CrossRef]
60. Weertman, J. Mechanism for the formation of inner moraines found near the edge of cold ice caps and ice sheets. *J. Glaciol.* **1961**, *3*, 965–978. [CrossRef]
61. Schulson, E.M. The brittle compressive fracture of ice. *Acta Metall. Mater.* **1990**, *38*, 1963–1976. [CrossRef]
62. Alsop, G.I.; Holdsworth, R.E. Flow perturbation folding in shear zones. In *Deformation of the Continental Crust: The Legacy of Mike Coward*; Ries, A.C., Butler, R.W.H., Graham, R.H., Eds.; Geological Society London Special Publications: London, UK, 2007; Volume 272, pp. 75–101. [CrossRef]
63. Grinsted, A.; Rathmann, N.M.; Mottram, R.; Solgaard, A.M.; Mathiesen, J.; Hvidberg, C.S. Failure strength of glacier ice inferred from Greenland crevasses. *Cryosphere* **2024**, *18*, 1947–1957. [CrossRef]
64. Petrovic, J.J. Review mechanical properties of ice and snow. *J. Mater. Sci.* **2003**, *38*, 1–6. [CrossRef]
65. Phillips, E.; Finlayson, A.; Jones, L. Fracturing, block faulting, and moulin development associated with progressive collapse and retreat of a maritime glacier: Falljökull, SE Iceland. *JGR Earth Surf.* **2013**, *118*, 1545–1561. [CrossRef]
66. Monz, M.E.; Hudleston, P.J.; Cook, S.J.; Zimmerman, T.; Leng, M.J. Thrust faulting in glaciers? Re-examination of debris bands near the margin of Storglaciären, Sweden. *Boreas* **2022**, *51*, 78–99. [CrossRef]
67. Herbst, P.; Neubauer, F. The Pasterze glacier, Austria: An analogue of an extensional allochthon. In *Deformation of Glacial Materials*; Maltman, A.J., Hubbard, B., Hambrey, M.J., Eds.; Geological Society London Special Publications: London, UK, 2000; Volume 176, pp. 159–168. [CrossRef]
68. Herbst, P.; Neubauer, F.; Schöpfer, M.P.J. The development of brittle structures in an alpine valley glacier: Pasterzenkees, Austria, 1887–1997. *J. Glaciol.* **2006**, *52*, 128–136. [CrossRef]

69. Fleming, E.J.; Lovell, H.; Stevenson, C.T.E.; Petronis, M.S.; Benn, D.I.; Hambrey, M.J.; Fairchild, I.J. Magnetic fabrics in the basal ice of a surge-type glacier. *JGR Earth Surf.* **2013**, *118*, 2263–2278. [CrossRef]
70. Hambrey, M.J.; Bennett, M.R.; Dowdeswell, J.A.; Glasser, N.F.; Huddart, D. Debris entrainment and transfer in polythermal valley glaciers. *J. Glaciol.* **1999**, *45*, 69–86. [CrossRef]
71. Hubbard, B.; Glasser, N.; Hambrey, M.; Etienne, J. A sedimentological and isotopic study of the origin of supraglacial debris bands: Kongsfjorden, Svalbard. *J. Glaciol.* **2004**, *50*, 157–170. [CrossRef]
72. Murray, T.; Booth, A.D. Imaging glacial sediment inclusions in 3-D using ground-penetrating radar at Kongsvegen, Svalbard. *J. Quat. Sci.* **2010**, *25*, 754–761. [CrossRef]
73. Bennett, M.R.; Hambrey, M.J.; Huddart, D.; Glasser, N.F.; Crawford, K. The landform and sediment assemblage produced by a tidewater glacier surge in Kongsfjorden, Svalbard. *Quat. Sci. Rev.* **1999**, *18*, 1213–1246. [CrossRef]
74. Hambrey, M.J.; Dowdeswell, J.A.; Murray, T.; Porter, P.R. Thrusting and debris-entrainment in a surging glacier: Bakaninbreen, Svalbard. *Geogr. Ann.* **1996**, *22*, 241–248. [CrossRef]
75. Hambrey, M.J.; Murray, T.; Glasser, N.F.; Hubbard, A.; Bubbard, B.; Stuart, G.; Hansen, S.; Kohler, J. Structure and changing dynamics of a polythermal valley glacier on a centennial timescale: Midre Lovenbreen, Svalbard. *J. Geophys. Res.* **2005**, *110*, F01006. [CrossRef]
76. Bennett, M.R. The morphology, structural evolution and significance of push moraines. *Earth Sci. Rev.* **2001**, *53*, 197–236. [CrossRef]
77. Bennett, M.R.; Huddart, D.; Waller, R.I.; Cassidy, N.; Tomio, A.; Zukowskyj, P.; Midgley, N.G.; Cook, S.J.; Gonzalez, S.; Glasser, N.F. Sedimentary and tectonic architecture of a large push moraine: A case study from Hagafellsjökull-Eystri, Iceland. *Sed. Geol.* **2004**, *172*, 269–292. [CrossRef]
78. Boulton, G.S.; Caban, P. Groundwater flow beneath ice sheets: Part II—Its impact on glacier tectonic structures and moraine formation. *Quat. Sci. Rev.* **1995**, *14*, 563–587. [CrossRef]
79. Collins, G.C.; McKinnon, W.B.; Moore, J.M.; Nimmo, F.; Pappalardo, R.T.; Prockter, L.M.; Schenk, P.M. Tectonics of the outer planet satellites. In *Planetary Tectonics*; Watters, T.R., Schultz, R.A., Eds.; Cambridge University Press: Cambridge, UK, 2009; Volume 11, p. 229.
80. Cameron, M.E.; Smith-Konter, B.R.; Collins, G.C.; Patthoff, D.A.; Pappalardo, R.T. Tidal stress modeling of Ganymede: Strike-slip tectonism and Coulomb failure. *Icarus* **2019**, *319*, 99–120. [CrossRef]
81. Rhoden, A.R.; Hurford, T.A.; Manga, M. Strike-slip fault patterns on Europa: Obliquity or polar wander? *Icarus* **2011**, *211*, 636–647. [CrossRef]
82. Shoemaker, E.M.; Lucchitta, B.K.; Wilhelms, D.E.; Plescia, J.B.; Squyres, S.W. The geology of Ganymede. In *Satellites of Jupiter*; Morrison, D., Ed.; The University of Arizona Press: Tucson, AZ, USA, 1982; pp. 435–520.
83. Collins, G.C.; Head, J.W., III; Pappalardo, R.T. Formation of Ganymede grooved terrain by sequential extensional episodes: Implications of Galileo observations for regional stratigraphy. *Icarus* **1998**, *135*, 345–359. [CrossRef]
84. Cameron, M.E.; Smith-Konter, B.R.; Burkhard, L.; Pappalardo, R.T.; Collins, G.C. Strike-slip faulting on Ganymede: Morphological mapping and failure mechanics. *Lunar Planet. Sci. Conf.* **2016**, *47*, 2630.
85. Cameron, M.E.; Smith-Konter, B.R.; Pappalardo, R.T.; Collins, G.; Nimmo, F. Tidally-driven strike slip failure mechanics on Ganymede. In Proceedings of the 44th Lunar and Planetary Science Conference (2013), Houston, TX, USA, 18–22 March 2013; p. 2711.
86. Cameron, M.E.; Smith-Konter, B.R.; Burkhard, L.; Collins, G.C.; Seifert, F.; Pappalardo, R.T. Morphological mapping of Ganymede: Investigating the role of strike-slip tectonics in the evolution of terrain types. *Icarus* **2018**, *315*, 92–114. [CrossRef]
87. Seifert, F.; Cameron, M.E.; Smith-Konter, B.R.; Pappalardo, R.T.; Collins, G.C. Global morphological mapping of strike-slip structures on Ganymede. In Proceedings of the 46th Lunar and Planetary Science Conference (2015), Houston, TX, USA, 16–20 March 2015; Volume 46.
88. Head, J.W.; Pappalardo, R.T.; Collins, G.C.; Belton, M.J.S.; Giese, B.; Wagner, R.; Breneman, H.; Spaun, N.; Nixon, B.; Neukum, G.; et al. Evidence for Europa-like tectonic resurfacing styles on Ganymede. *Geop. Res. Lett.* **2002**, *29*, 4-1–4-4. [CrossRef]
89. Murchie, S.L.; Head, J.W. Possible breakup of dark terrain on Ganymede by large-scale shear faulting. *J. Geophys. Res.* **1988**, *93*, 8795–8824. [CrossRef]
90. Bedle, H.; Jurdy, D.M. Ganymede's sulci on global and regional scales. In Proceedings of the Lunar and Planetary Science XXXVI (2005), League City, TX, USA, 14–18 March 2005; p. 1161.
91. Berquin, Y.; Kofman, W.; Herique, A.; Alberti, G.; Beck, P. A study on Ganymede's surface topography: Perspectives for radar sounding. *Planet. Space Sci.* **2013**, *77*, 40–44. [CrossRef]
92. Schenk, P.M.; McKinnon, W.B. Fault offsets and lateral crustal movement on Europa: Evidence for a mobile ice shell. *Icarus* **1989**, *79*, 75–100. [CrossRef]
93. Prockter, L.M.; Head, J.W., III; Pappalardo, R.T.; Sullivan, R.J.; Clifton, A.E.; Giese, B.; Wagner, R.; Neukum, G. Morphology of Europan bands at high resolution: A mid-ocean ridge-type rift mechanism. *JGR Planets* **2002**, *107*, 4-1–4-26. [CrossRef]

94. Greeley, R.; Chyba, C.F.; Head, J.W.; McCord, T.B.; McKinnon, W.B.; Pappalardo, R.T.; Figueredo, P.H. Geology of Europa. In *Jupiter: The Planet, Satellites and Magnetosphere*; Bagenal, F., Dowling, T.E., McKinnon, W.B., McKinnon, W., Eds.; Cambridge University Press: Cambridge, UK, 2004; pp. 329–362.
95. Hoppa, G.V.; Tufts, B.R.; Greenberg, R.; Geissler, P.E. Formation of cycloidal features on Europa. *Science* **1999**, *285*, 1899–1902. [CrossRef] [PubMed]
96. Prockter, L.M.; Pappalardo, A.R.T. Folds on Europa: Implications for crustal cycling and accommodation of extension. *Science* **2000**, *289*, 941–943. [CrossRef] [PubMed]
97. Kattenhorn, S.A.; Prockter, L.M. Evidence for subduction in the ice shell of Europa. *Nat. Geosci.* **2014**, *7*, 762–767. [CrossRef]
98. Hoppa, G.; Greenberg, R.; Tufts, B.R.; Geissler, P.; Phillips, C.; Milazzo, M. Distribution of strike-slip faults on Europa. *JGR Planets* **2000**, *105*, 22617–22627. [CrossRef]
99. Tufts, B.R.; Greenberg, R.; Hoppa, G.; Geissler, P. Astypalaea Linea: A large-scale strike-slip fault on Europa. *Icarus* **1999**, *141*, 53–64. [CrossRef]
100. Kattenhorn, S.A. Strike-slip fault evolution on Europa: Evidence from tailcrack geometries. *Icarus* **2004**, *172*, 582–602. [CrossRef]
101. Greenberg, R. The evil twin of Agenor: Tectonic convergence on Europa. *Icarus* **2004**, *167*, 313–319. [CrossRef]
102. Geissler, P.E.; Greenberg, R.; Hoppa, G.; McEwen, A.; Tufts, R.; Phillips, C.; Clark, B.; Ockert-Bell, M.; Helfenstein, P.; Burns, J.; et al. Evolution of lineaments on Europa: Clues from Galileo multispectral imaging observations. *Icarus* **1998**, *135*, 107–126. [CrossRef]
103. Crow-Willard, E.N.; Pappalardo, R.T. Structural mapping of Enceladus and implications for formation of tectonized regions. *JGR Planets* **2015**, *120*, 928–950. [CrossRef]
104. Porco, C.C.; Helfenstein, P.; Thomas, P.C.; Ingersoll, A.P.; Wisdom, J.; West, R.; Neukum, G.; Denk, T.; Wagner, R.; Roatsch, T.; et al. Cassini observes the active south pole of Enceladus. *Science* **2006**, *311*, 1393–1401. [CrossRef] [PubMed]
105. Tajeddine, R.; Soderlund, K.M.; Thomas, P.C.; Helfenstein, P.; Hedman, M.M.; Burns, J.A.; Schenk, P.M. True polar wander of Enceladus from topographic data. *Icarus* **2017**, *295*, 46–60. [CrossRef]
106. Nimmo, F.; Pappalardo, R.T. Furrow flexure and ancient heat flux on Ganymede. *Geoph. Res. Lett.* **2004**, *31*, L19701. [CrossRef]
107. Pappalardo, R.T.; Davis, D.M. Where's the compression? Explaining the lack of contractional structures on icy satellites. *Workshop Ices Ocean. Fire Satell. Outer Sol. Syst.* **2007**, *1357*, 108–109.
108. Lucchetti, A.; Dalle Ore, C.; Pajola, M.; Pozzobon, R.; Rossi, C.; Galluzzi, V.; Penasa, L.; Stephan, K.; Munaretto, G.; Cremonese, G.; et al. Geological, compositional and crystallinity analysis of the Melkart impact crater, Ganymede. *Icarus* **2023**, *401*, 115613. [CrossRef]
109. Jones, C.; Ryan, J.; Holt, T.; Hubbard, A. Structural glaciology of Isunguata Sermia, West Greenland. *J. Maps* **2018**, *14*, 517–527. [CrossRef]
110. Rippin, D.M.; Pomfret, A.; King, N. High resolution mapping of supra-glacial drainage pathways reveals link between micro-channel drainage density, surface roughness and surface reflectance. *Earth Sur. Proc. Land.* **2015**, *40*, 1279–1290. [CrossRef]
111. Hodgetts, D. Virtual Reality Geological Studio. 2019. Available online: https://www.vrgeoscience.com (accessed on 1 March 2025).
112. Haslebacher, C.; Thomas, N.; Bickel, V.T. LineaMapper: A deep learning-powered tool for mapping linear surface features on Europa. *Icarus* **2024**, *410*, 115722. [CrossRef]
113. Kersten, E.; Zubarev, A.E.; Roatsch, T.; Matz, K.D. Controlled global Ganymede mosaic from voyager and Galileo images. *Plan. Space Sci.* **2021**, *206*, 105310. [CrossRef]
114. Orheim, O.; Lucchitta, B.K. Snow and ice studies by thematic mapper and multispectral scanner Landsat images. *Ann. Glaciol.* **1987**, *9*, 109–118. [CrossRef]
115. Yu, J.; Liu, H.; Wang, L.; Jezek, K.C.; Heo, J. Blue ice areas and their topographical properties in the Lambert glacier, Amery Iceshelf system using Landsat ETM+, ICESat laser altimetry and ASTER GDEM data. *Antarct. Sci.* **2012**, *24*, 95–110. [CrossRef]
116. Woodward, J.; Murray, T.; Clark, R.A.; Stuart, G.W. Glacier surge mechanisms inferred from ground-penetrating radar: Kongsvegen, Svalbard. *J. Glaciol.* **2003**, *49*, 473–480. [CrossRef]
117. Plewes, L.A.; Hubbard, B. A review of the use of radio-echo sounding in glaciology. *Progr. Phys. Geogr.* **2001**, *25*, 203–236. [CrossRef]
118. Grasset, O.; Dougherty, M.K.; Coustenis, A.; Bunce, E.J.; Erd, C.; Titov, D.; Blanc, M.; Coates, A.; Drossart, P.; Fletcher, L.N.; et al. JUpiter ICy moons explorer (JUICE): An ESA mission to orbit Ganymede and to characterise the Jupiter system. *Planet. Space Sci.* **2013**, *78*, 1–21. [CrossRef]
119. Howell, S.M.; Pappalardo, R.T. NASA's Europa Clipper—A mission to a potentially habitable ocean world. *Nat. Commun.* **2020**, *11*, 1311. [CrossRef]

120. Bruzzone, L.; Plaut, J.J.; Alberti, G.; Blankenship, D.D.; Bovolo, F.; Campbell, B.A.; Seu, R. RIME: Radar for icy moon exploration. In Proceedings of the 2013 IEEE International Geoscience and Remote Sensing Symposium—IGARSS, Melbourne, VIC, Australia, 21–26 July 2013; pp. 3907–3910.
121. Blankenship, D.; Ray, T.; Plaut, J.; Moussessian, A.; Patterson, W.; Romero-Wolf, A.; REASON Science Team. REASON for Europa. In Proceedings of the 42nd Cospar Scientific Assembly, Pasadena, CA, USA, 14–22 July 2018; Volume 42, p. B5-3.

Disclaimer/Publisher's Note: The statements, opinions and data contained in all publications are solely those of the individual author(s) and contributor(s) and not of MDPI and/or the editor(s). MDPI and/or the editor(s) disclaim responsibility for any injury to people or property resulting from any ideas, methods, instructions or products referred to in the content.